International Journal of Advance Research and Innovation
Vol. 4(1), Jan-Mar 2016, pp. 219-229
Doi: 10.51976/ijari.411632

Article Info
Received: 01 Jan 2016 | Revised Submission: 20 Feb 2016 | Accepted: 01 Mar 2016 | Available Online: 01 Jun 2016

Effect of aspect ratio on the performance and stability of Hydrodynamic Journal Bearings

Sanjay Sharma and R K Awasthi***

ABSTRACT

The purpose of this paper is to theoretically study the effect of aspect ratio on the performance of fluid-film bearing system .Based upon the dynamic Reynolds governing equation for the different aspect ratio, the various performance parameters: eccentricity ratio, maximum pressure, coefficient of friction, minimum film thickness, attitude angle, direct and cross-coupled stiffness and damping coefficients, threshold speed, whirl-frequency ratio and critical mass of hydrodynamic journal bearings are evaluated. The aspect ratios (L/D) are considered 0.5, 1.0 and 1.5 for the analysis of purpose. The influence of L/D ratio on bearing performance parameters for a wide range of Somerfield number has been presented. The results could be useful to give more insight to bearing designer for predicting a suitable L/D ratio for enhanced stable bearing operations.

Keywords: *Hydrodynamic Journal Bearing; FEM; Aspect Ratio.*

1.0 Introduction

Hydrodynamic journal bearing are useful in rotating machinery for supporting radial loads. These bearings allow for transmission of large loads at mean speed of rotation and are susceptible to large amplitude lateral vibration due to self exited instability which is known as oil whirl or synchronous whirl. Under certain unexpected disturbances the bearing system is prone to an oscillating behavior.

If the amplitude of oscillation grows too much, it may cause the undesired journal-bearing contact and endanger safe operation of the whole machine system. The important parameters such as surface roughness, fluid inertia, rehology of lubricant and bearing size (aspect ratio) and geometry may have an influence on bearing performance and its stability.

Many researchers [1-9] have theoretically investigated the performance and stability of hydrodynamic journal bearings. Owing to various influencing factors Zhang, et al. [1] considered the effect of L/D ratio and slip on the stability analysis of gas-lubricated journal bearing in micro-electro-mechanical systems (MEMS). Das, et al. [2] used first order perturbation for dynamic characteristics of hydrodynamic bearing with respect to micropolar property for varying eccentricity ratios and L/D ratios. Osman, et al. [3] studied the static and dynamic characteristics of the magnetized journal bearings lubricated with ferrofluids.

By using finite perturbation technique, the eight-oil film stiffness and damping coefficients were determined with L/D ratio as 1.0. Zhang, et al. [4] determined the stiffness coefficient of hydrodynamic plain journal bearings lubricated with water.

The relationship between the stiffness coefficients and the load for bearing with different relative clearance, different L/D ratios and different rotational speed are obtained. Singhal and Khonsari [5] investigated the stability of a journal bearing system, including the effects of inlet viscosity.

Simplified thermo-hydrodynamic design charts for the rapid prediction of stiffness coefficients, damping coefficients, and threshold speed have been developed. Jang and Yoon [6] presented analytical method to investigate the stability of a hydro dynamic journal bearing with rotating herringbone grooves.

The dynamic coefficients of the hydro dynamic journal bearing are calculated using the FEM and perturbation method. Sharma and Krishna [7] considered the effect of L/D ratio on the dynamic performance characteristics and stability of two-lobe pressure dam bearing. Dwivedi, et al. [8] theoretically computed the static and dynamic performance parameters of hydrodynamic bearing considering

**Corresponding Author: Department of Mechanical Engineering, Shri Mata Vaishno Devi University Katra, India (E-mail: sanjufrnd15@gmail.com)*
***Department of Mechanical Engineering, Beant College of Engineering and Technology, Gurdaspur, Punjab, India (E-mail: awasthi.rka@gmail.com)*

short bearing approximation aspect ratio (L/D < 0.5) under different flow regime. Mehta, et al. [9] analysed the static and dynamic performance parameters of a four-lobe pressure-dam bearing which is produced by incorporating two pressure dams on the upper two lobes and two lobes and two relief-tracks on the lower two lobes of an ordinary four- lobe bearing with L/D ratio as 1.0

A study of bearing dynamics is important for enhancing smooth bearing life. An understanding on how bearing size (aspect ratio) influences bearing performance in particular bearing dynamics is still not been fully revealed.

The current study has been undertaken with the objective of through understanding about the role of aspect ratio on static, dynamic and stability aspect of fluid-film journal bearing. Thus the current study presents the influence of aspect ratio on bearing performance for a wide range of sommerfeld number.

2.0 Theory

The conventional Reynolds equation for an incompressible, Newtonian lubricant in the clearance space of a finite journal bearing system is given below in non-dimensional form as [16]:

$$\frac{\partial}{\partial\alpha}\left(\frac{\bar{h}^3}{12}\frac{\partial\bar{p}}{\partial\alpha}\right)+\frac{\partial}{\partial\beta}\left(\frac{\bar{h}^3}{12}\frac{\partial\bar{p}}{\partial\beta}\right)=\frac{\Omega}{2}\frac{\partial\bar{h}}{\partial\alpha}+\frac{\partial\bar{h}}{\partial\tau} \quad (1)$$

The conventional Reynolds Eq. (1) is solved using FEM, which is described below.

2.1 FEM Formulation

The weighted residual of Eq. (1) using Galerkin's criteria may be expressed as [16]:

$$\iint_{A^e}\left\{\frac{\partial}{\partial\alpha}\left(\frac{\bar{h}^3}{12}\frac{\partial\bar{p}^e}{\partial\alpha}\right)+\frac{\partial}{\partial\beta}\left(\frac{\bar{h}^3}{12}\frac{\partial\bar{p}^e}{\partial\alpha}\right)-\frac{\Omega}{2}\frac{\partial\bar{h}}{\partial\alpha}-\frac{\partial\bar{h}}{\partial\tau}\right\}N_i d\alpha d\beta=0 \quad (2)$$

where N_i is the interpolation function relating the nodal pressures $\bar{p}_j$ to the pressure in the e[th] element of the discretized pressure field of N finite elements, i.e.,

$$\bar{p}^e=\sum_{j=1}^{n^e}N_j\bar{p}_j \quad (3)$$

where N_j is the elemental shape function and n^e is number of nodes per element of two-dimensional flow-field discretized solution domain. With simplifications, Eqs. (2) and (3) give the element Eq. as [16]:

$$\left[\bar{F}^e\right]_{n^e\times n^e}\left\{\bar{p}^e\right\}_{n^e\times 1}=\left\{\bar{Q}^e\right\}_{n^e\times 1}+\Omega\left\{\bar{R}_H^{\ e}\right\}_{n^e\times 1}+\dot{\bar{x}}\left\{\bar{R}_{X_j}^{\ e}\right\}_{n^e\times 1}+\dot{\bar{z}}\left\{\bar{R}_{Z_j}^{\ e}\right\}_{n^e\times 1} \quad (4)$$

where $\dot{x}$ and $\dot{z}$ are the journal centre velocity.

For an e^{th} element, the elements of the above matrices are defined as follows [16]:

$$\bar{F}_{ij}^{\ e}=\iint_{A^e}\bar{h}^3\left[\frac{1}{12}\frac{\partial N_i}{\partial\alpha}\frac{\partial N_j}{\partial\alpha}+\frac{1}{12}\frac{\partial N_i}{\partial\beta}\frac{\partial N_j}{\partial\beta}\right]d\alpha\,d\beta \quad (5)$$

$$\bar{Q}_i^{\ e}=\int_{\Gamma^e}\left\{\left(\frac{\bar{h}^3}{12}\frac{\partial\bar{p}^e}{\partial\alpha}-\frac{\Omega\bar{h}}{2}\right)l+\left(\frac{\bar{h}^3}{12}\frac{\partial\bar{p}}{\partial\beta}\right)m\right\}N_i d\bar{\Gamma}^e \quad (6)$$

$$\bar{R}_{H_i}^{\ e}=\iint_{A^e}\frac{\bar{h}}{2}\frac{\partial N_i}{\partial\alpha}d\alpha\,d\beta \quad (7)$$

$$\bar{R}_{X_{J_i}}^{\ e}=\iint_{A^e}N_i\cos\alpha\,d\alpha\,d\beta \quad (8)$$

$$\bar{R}_{Z_{J_i}}^{\ e}=\iint_{A^e}N_i\sin\alpha\,d\alpha\,d\beta \quad (9)$$

where l and m are the directions cosines and i, j =1,2 … n^e .

The assembly of Eq. (4) over the entire domain of pressure field results in global linear equations

$$\left[\bar{F}\right]_{N\times N}\left\{\bar{p}\right\}_{N\times 1}=\left\{\bar{Q}\right\}_{N\times 1}+\Omega\left\{\bar{R}_H\right\}_{N\times 1}+\dot{\bar{x}}\left\{\bar{R}_{X_J}\right\}_{N\times 1}+\dot{\bar{z}}\left\{\bar{R}_{Z_J}\right\}_{N\times 1} \quad (10)$$

involving two sets of nodal variables, the pressure $\{\bar{p}\}$ and the flow $\{\bar{Q}\}$.

2.2 Boundary conditions

The boundary condition used for the solution of lubricant flow field are described as:

$$P=0\ ,\ at\ \frac{\partial p}{\partial\alpha}=0 \quad (11)$$

Eq. (10) can be solved to give both pressure and flow simultaneously because at each node one of the two variables is known.

Fig.1 shows the coordinate and the schematic of a simple plain journal bearing in a steady-state configuration. The static performance characteristics are computed for the steady-state condition, $\text{i.e.,}\ \dot{\bar{x}} = \dot{\bar{z}} = 0$. For the computation of performance characteristics, it is essential to establish the journal center equilibrium position for a given vertical load. The solution process is expressed in flow chart shown in fig.2.

Fig. 1. Definition of the Coordinate and the Schematic of A Simple Plain Journal Bearing.

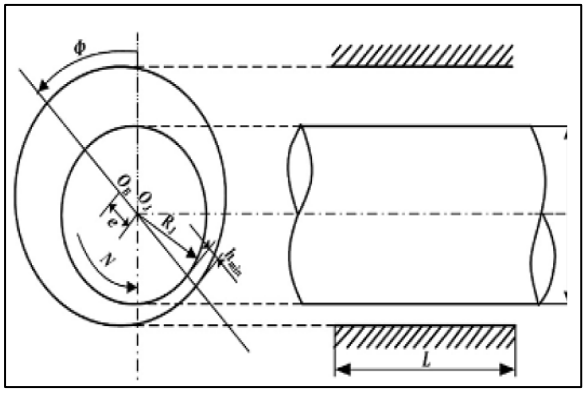

2.3 Journal Center Equilibrium Position

For a given vertical external load $\overline{W}_o$ or eccentricity ratio and operating and geometric parameters of the bearing, the journal center position $(\overline{X}_J, \overline{Z}_J)$ is unique. This journal center equilibrium position is not known a priori and is obtained iteratively. For a specified vertical external load $(\overline{W}_o)$, which acts parallel to the Z-axis and when the journal center occupies its equilibrium positions, the fluid-film reaction components must satisfy the following conditions [16].

$$\left.\begin{aligned} \overline{F}_x &= 0 \\ \overline{F}_z - \overline{W}_o &= 0 \end{aligned}\right\} \qquad (12)$$

Initially the tentative values of journal center coordinates ($\overline{X}_J, \overline{Z}_J$) are fed as input to compute the nominal fluid-film thickness $(\overline{h})$ that is required for the computation of fluid-film pressures. The fluid-film reaction components $\overline{F}_x$ and $\overline{F}_z$ are computed using Eqs. (13) and (14), respectively.

2.4 Load Carrying Capacity $(\overline{F})$

Fluid-film reaction components along *X* and *Z* directions are respectively given by [12, 13]

$$\overline{F}_x = -\int_{-\lambda}^{\lambda}\int_{0}^{2\pi} \overline{p}\cos\alpha \, d\alpha \, d\beta \qquad (13)$$

and

$$\overline{F}_z = -\int_{-\lambda}^{\lambda}\int_{0}^{2\pi} \overline{p}\sin\alpha \, d\alpha \, d\beta \qquad (14)$$

Then, the resultant fluid-film reaction is expressed as

$$\overline{F} = \left[\overline{F}_x^2 + \overline{F}_z^2\right]^{1/2} \qquad (15)$$

2.5 Nominal Minimum Fluid-Film Thickness ($\overline{h}_{\min}$)

Using the computed journal center coordinates ($\overline{X}_J$ and $\overline{Z}_J$), the minimum fluid-film thickness [14, 15] and eccentricity ratio are computed from the expressions given below:

$$\overline{h} = \overline{h}_0 = 1 - \overline{X}_J\cos\alpha - \overline{Z}_J\sin\alpha \qquad (16)$$

The eccentricity ratio is given by

$$\varepsilon = \sqrt{\left|\overline{X}_J\right|^2 + \left|\overline{Z}_J\right|^2} \qquad (17)$$

2.6 Sommerfeld Number

The characteristics in steady running of a journal bearing of specified design are usually expressed non-dimensionally as functions of a single parameter called the Sommerfeld Number [10].The Sommerfeld Number can be determined as:

$$S = \frac{2\left(\frac{L}{D}\right)}{\pi \bar{W}} \qquad (18)$$

2.7 Attitude Angle (ϕ)

The angle between the line joining bearing, journal center and load line is defined as attitude angle. The attitude angle, ϕ is calculated by [16]:

$$\phi = \tan^{-1}\left[\frac{\bar{X}_J}{\bar{Z}_J}\right] \qquad (19)$$

For different positions of journal centre, the expressions to the attitude angle will be different.

2.8 Friction power loss $(\bar{P}_L)$

The power loss/ torque in a journal bearing is computed from the following equation [16]:

$$\bar{P}_L = \sum_{e=1}^{n_e} \int_{A^e} \left(\Omega \frac{\bar{\tau}_c}{\bar{h}} + \frac{\bar{h}}{2} \frac{\partial \bar{p}}{\partial \alpha} \right) dA \qquad (20)$$

where $\bar{\tau}_c$ is the normalized turbulent couette shearing stress.

A journal bearing system has two degrees of freedom to define the journal position during its oscillation. Considering two degrees of freedom system, 2x2 fluid-film stiffness and 2x2 fluid-film damping coefficients can be computed using the expressions given below.

2.9 Fluid-Film Stiffness Coefficients

The fluid-film stiffness coefficients are defined as [16]:

$$\bar{S}_{ij} = -\frac{\partial \bar{F}_i}{\partial \bar{q}_J}, (i = x, z) \qquad (21)$$

Where,

i = direction of force.

$\bar{q}_J$ = direction of journal center displacement ($\bar{q}_J = \bar{x}, \bar{z}$).

Stiffness coefficient matrix will be

$$\begin{bmatrix} \bar{S}_{xx} & \bar{S}_{xz} \\ \bar{S}_{zx} & \bar{S}_{zz} \end{bmatrix} = -\begin{bmatrix} \frac{\partial \bar{F}_x}{\partial \bar{x}} & \frac{\partial \bar{F}_x}{\partial \bar{z}} \\ \frac{\partial \bar{F}_z}{\partial \bar{x}} & \frac{\partial \bar{F}_z}{\partial \bar{z}} \end{bmatrix} \qquad (22)$$

2.10 Fluid-Film Damping Coefficients

The fluid-film damping coefficients are defined as [16]:

$$\bar{C}_{ij} = -\frac{\partial \bar{F}_i}{\partial \dot{\bar{q}}_J}, (i = x, z) \qquad (23)$$

$\dot{q}$ represents the velocity component of journal center ($\dot{\bar{x}}, \dot{\bar{z}}$).

Damping coefficients matrix is given by:

$$\begin{bmatrix} \bar{C}_{xx} & \bar{C}_{xz} \\ \bar{C}_{zx} & \bar{C}_{zz} \end{bmatrix} = -\begin{bmatrix} \frac{\partial \bar{F}_x}{\partial \dot{\bar{x}}} & \frac{\partial \bar{F}_x}{\partial \dot{\bar{z}}} \\ \frac{\partial \bar{F}_z}{\partial \dot{\bar{x}}} & \frac{\partial \bar{F}_z}{\partial \dot{\bar{z}}} \end{bmatrix} \qquad (24)$$

2.11 Critical mass

The non-dimensional critical mass $\bar{M}_c$ of the journal is expressed as [16]:

$$\bar{M}_c = \frac{\bar{G}_1}{\bar{G}_2 - \bar{G}_3} \qquad (25)$$

Where,

$$\bar{G}_1 = \left[\bar{C}_{xx}\bar{C}_{zz} - \bar{C}_{zx}\bar{C}_{xz}\right],$$

$$\bar{G}_2 = \frac{\left[\bar{S}_{xx}\bar{S}_{zz} - \bar{S}_{zx}\bar{S}_{xz}\right]\left[\bar{C}_{xx} + \bar{C}_{zz}\right]}{\left[\bar{S}_{xx}\bar{C}_{zz} + \bar{S}_{zz}\bar{C}_{xx} - \bar{S}_{xz}\bar{C}_{zx} - \bar{S}_{zx}\bar{C}_{xz}\right]} \quad \text{and}$$

$$\bar{G}_3 = \frac{\left[\bar{S}_{xx}\bar{C}_{xx} + \bar{S}_{xz}\bar{C}_{xz} + \bar{S}_{zx}\bar{C}_{zx} + \bar{S}_{zz}\bar{C}_{zz}\right]}{\left[\bar{C}_{xx} + \bar{C}_{zz}\right]}$$

2.12 Threshold speed

The speed of journal at the threshold of instability, can be obtained by [15, 16]:

$$\bar{\omega}_{th} = \left[\bar{M}_c \Big/ \bar{F}_o\right]^{1/2} \qquad (26)$$

Where, $\bar{F}_0$ is the resultant fluid-film force or reaction $\left(\frac{\partial \bar{h}}{\partial \bar{t}} = 0\right)$.A journal bearing system is asymptotically stable when the journal mass $\bar{M}_J$ is less than the critical mass $\bar{M}_c$ (i.e. when $\bar{M}_J < \bar{M}_c$). Likewise, a system is asymptotically stable when the operating speed of the journal is less than the threshold speed (i.e. when $\Omega < \bar{\omega}_{th}$).

2.13 Whirl frequency ratio

Whirl frequency ratio $\overline{\omega}_{whirl}$ can be expressed in simplified form as [15, 16]:

$$\overline{\omega}_{whirl}{}^{2} = \frac{K_1}{\overline{M}_c} \qquad (27)$$

Where, K_1 is expressed as:

$$K_1 = \frac{\overline{S}_{xx}\overline{C}_{zz} + \overline{S}_{zz}\overline{C}_{xx} - \overline{S}_{xz}\overline{C}_{zx} - \overline{S}_{zx}\overline{C}_{xz}}{\overline{C}_{xx} + \overline{C}_{zz}}$$

The lower the value of $\overline{\omega}_{whirl}$, the higher will be stability.

The negative value of $\overline{\omega}^{2}_{whirl}$ implies the absence of the whirl.

The simulated data for non dimensional bearing performance parameters have been generated and plotted to gain understanding. The results have been discussed in the following paragraphs.

3.0 Result and Discussion

The present results for hydrodynamic journal bearing as shown in fig.3 shows the variation of eccentricity ratio with respect to Sommerfeld number for varying L/D ratio. Figure shows that the bearing with L/D ratio of 0.5 has higher eccentricity ratio than other L/D ratios. It is observed that the increase in L/D ratio decrease the eccentricity ratio (i.e increases the load capacity). The similar reduction trend in the value of eccentricity ratio was reported in ref. [8, 11].

Fig. 3: Eccentricity Ratio Versus Sommerfeld Number

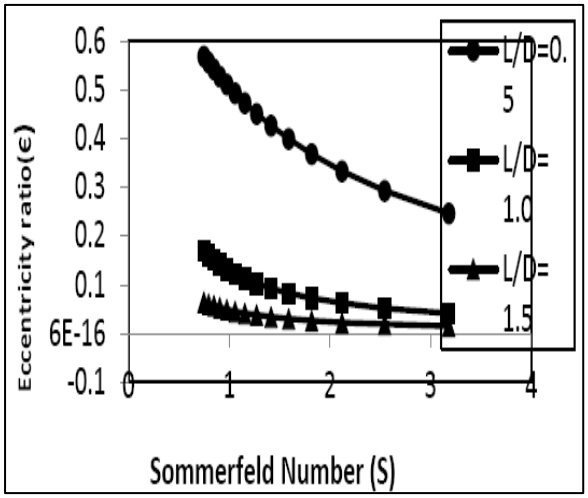

Fig. 4 shows the variation of maximum pressure with respect to Sommerfeld number for varying L/D ratio. Figure shows that the bearing with L/D ratio of 0.5 has higher maximum pressure than other L/D ratios. It is observed that the value of maximum pressure for a specified Sommerfeld number decreases with the increases in L/D ratio. The similar reduction trend in the value of maximum pressure was reported in ref. [11].

Fig. 5 shows the variation of minimum fluid-film thickness with respect to Sommerfeld number for varying L/D ratio. It is observed that the value of minimum fluid-film thickness for a specified Sommerfeld number increases with the increases in L/D ratio. The reduction in the value of fluid-film thickness is quite significant at lower L/D ratio of 0.5.

The similar reduction trend in the value of $\overline{h}_{\min}$ was reported in ref. [8, 9]

The variation of attitude angle with respect to Sommerfeld number for different values of L/D ratios, is shown in Fig.6. Attitude angle increases with increases in Sommerfeld number and L/D ratio. Figure also shows that the change in the values of attitude angle at L/D ratio of 0.5 has more variation with other L/D ratios.

The similar trend in the value of attitude angle was reported in in ref. [7,8].

The variation of friction coefficient with respect to Sommerfeld number for varying L/D ratio is shown in fig.7 Friction coefficient is increased with increasing L/D ratio. The behavior of coefficient of friction with different L/D ratios is similar as in ref.[9,11].

The results shows, that there is judicious need to select optimal L/D ratio from the view point of frictional power loss and load carrying capacity of fluid film journal bearing.

Figure 8, 9 shows the results for dimensionless direct stiffness coefficient parameters ($\overline{S}_{xx}$ and $\overline{S}_{zz}$) with respect to Sommerfeld number. The bearing configuration L/D equals to 0.5, 1.0 and 1.5. The direct fluid-film stiffness coefficients $\overline{S}_{xx}$ and $\overline{S}_{zz}$ as shown in fig.8 and fig.9 shows a decreasing trend with an increase in L/D ratio. The behavior of direct fluid-film stiffness coefficients $\overline{S}_{xx}$ and $\overline{S}_{zz}$ with different L/D ratios is similar as in ref.[8,11]. The fig.9 indicates that for same value of external vertical load, the vertical deformation in fluid-film is less corresponding to L/D ratio equals to 0.5, indicate better stability.

Fig. 2: Overall solution scheme

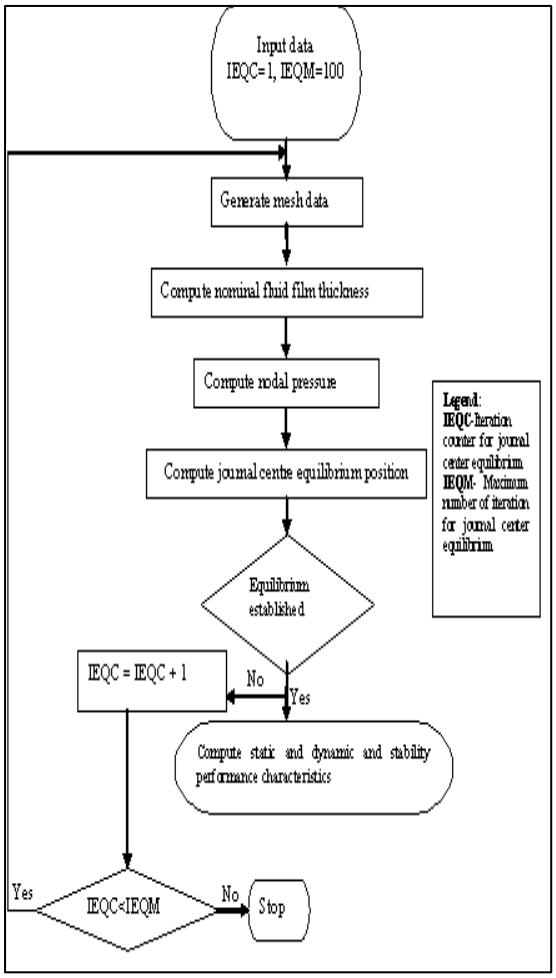

Fig.4 : Maximum Pressure Versus Sommerfeld Number

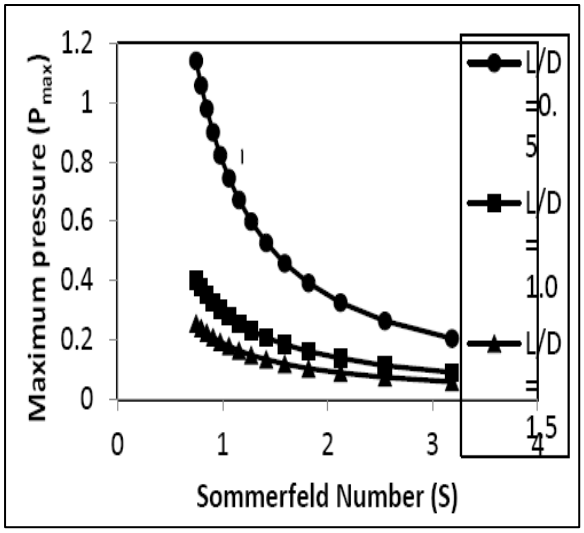

Fig. 5: Minimum fluid-film thickness versus Sommerfeld number

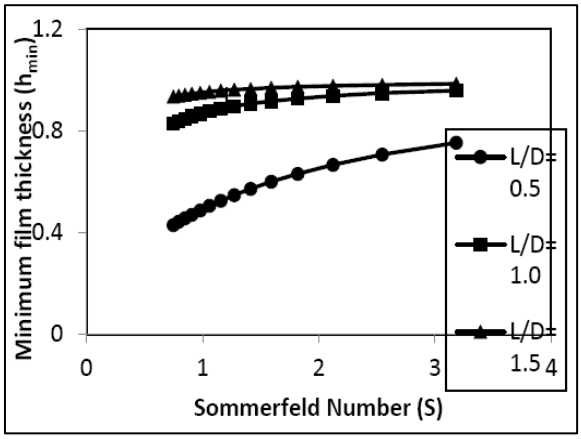

Fig. 6: Attitude angle versus Sommerfeld number

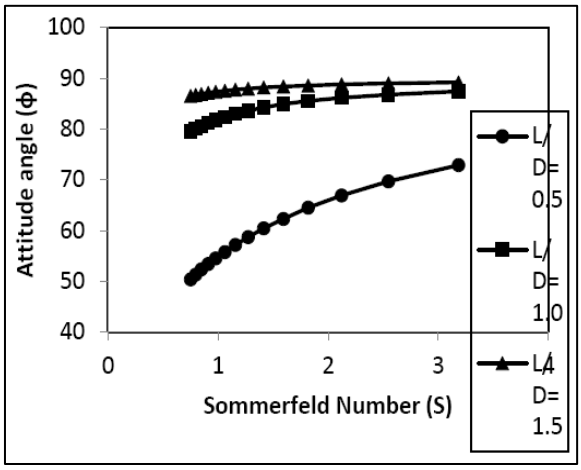

Fig. 7: Coefficient of Friction Versus Sommerfeld Number

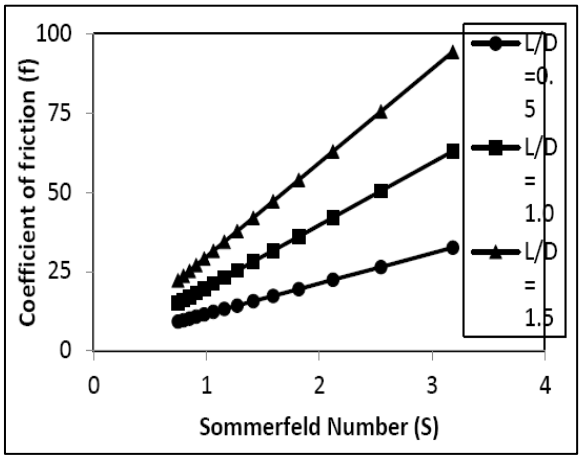

Fig. 8: Direct Fluid-Film Stiffness Coefficient Versus Sommerfeld Number

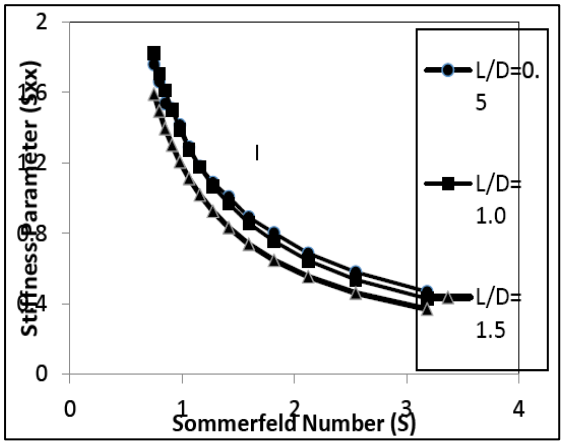

Fig.9: Direct Fluid-Film Stiffness Coefficient Versus Sommerfeld Number

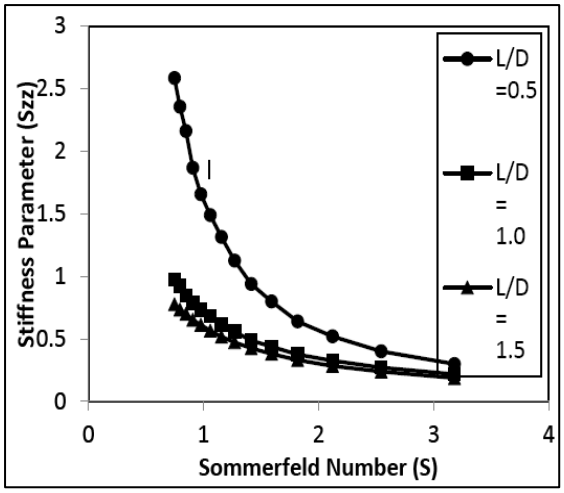

Fig. 10: Cross-Coupled Fluid-Film Stiffness Coefficient Versus Sommerfeld Number

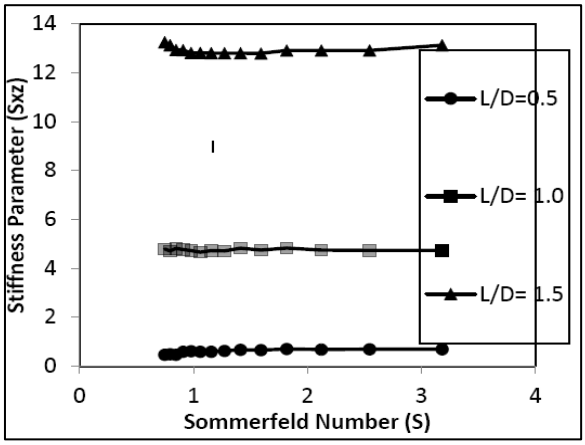

Fig. 11: Cross-Coupled Fluid-Film Stiffness Coefficient Versus Sommerfeld Number

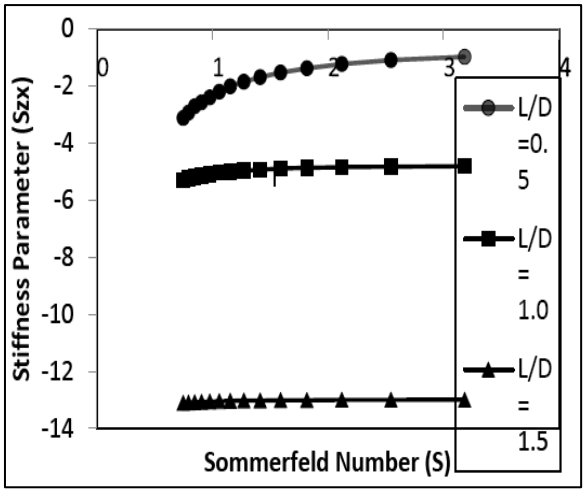

Figure 10, 11 shows the results for dimensionless cross coupled fluid-film stiffness coefficient ($\overline{S}_{xz}$ and $\overline{S}_{zx}$) with respect to Sommerfeld number. The bearing configuration L/D equals to 0.5, 1.0 and 1.5. The dimensionless value of cross coupled fluid-film stiffness coefficients $\overline{S}_{xz}$, as shown in fig 10 increases with an increase in L/D ratio and The dimensionless value of cross coupled fluid-film stiffness coefficients $\overline{S}_{zx}$ as shown in fig 11 decreases with increase in L/D ratio. The cross coupled fluid-film stiffness coefficient $\overline{S}_{zx}$ shows negative trend. The similar trend in the value of cross coupled fluid-film stiffness coefficients $\overline{S}_{xz}$ and $\overline{S}_{zx}$ was reported in ref. [8,11].

Figure 12 and 13 shows the results for direct dimensionless damping coefficient parameters($\overline{C}_{xx}$ and $\overline{C}_{zz}$) with respect to Sommerfeld number .The bearing configuration L/D equals to 0.5, 1.0 and 1.5.The direct dimensionless damping coefficient parameters $\overline{C}_{xx}$ and $\overline{C}_{zz}$ as shown in fig.12 and fig.13 shows an increasing trend with an increase in L/D ratio. The value of direct fluid-film damping coefficients $\overline{C}_{xx}$ and $\overline{C}_{zz}$ is constant at lower value of Sommerfeld number and decreases with an increase in the value of Sommefeld number. The behavior of dimensionless damping coefficient parameters $\overline{C}_{xx}$ and $\overline{C}_{zz}$ with different L/D ratios is similar as in ref. [8, 11].

Fig.12: Direct Fluid-Film Damping Coefficient Versus Sommerfeld Number

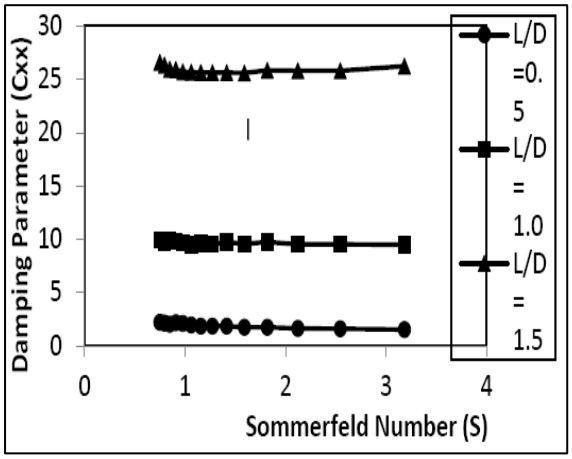

Fig. 13: Direct Fluid-Film Damping Coefficient Versus Sommerfeld Number

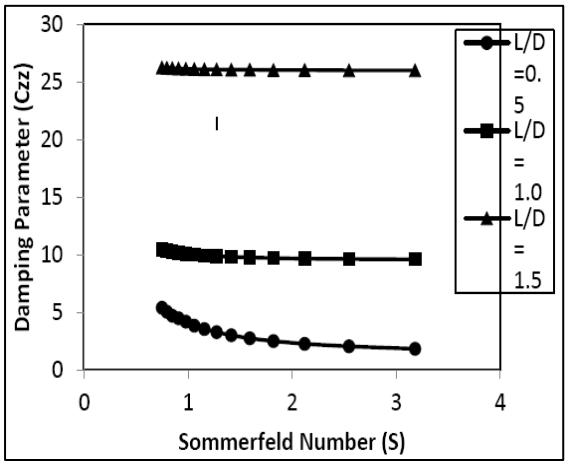

Figure 14 shows the results for cross coupled fluid-film dimensionless damping coefficient parameters ($\overline{C}_{xz}$ *and* $\overline{C}_{zx}$) with respect to Sommerfeld number. The bearing configuration L/D equals to 0.5, 1.0 and 1.5. The cross coupled fluid-film dimensionless damping coefficient parameters $\overline{C}_{xz}$ and $\overline{C}_{zx}$ as shown in fig.14 shows a decreasing trend with an increase in L/D ratio and shows negative behavior. The behavior of cross coupled fluid-film dimensionless damping coefficients $\overline{C}_{xz}$ and $\overline{C}_{zx}$ with different L/D ratios is similar as in ref. [8,11].

Fig. 14: Cross-Coupled Fluid-Film Damping Coefficient Versus Sommerfeld Number

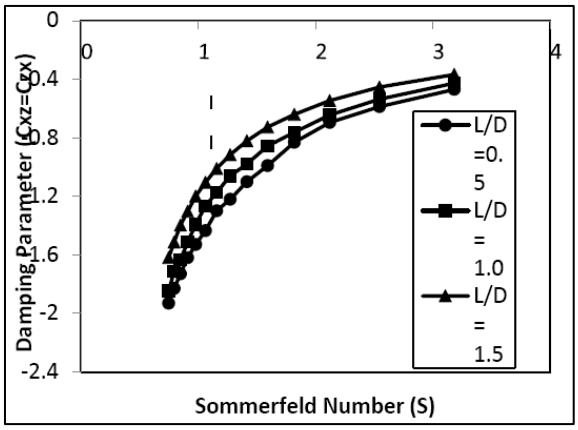

Variation of the whirl frequency ratio with Sommerfeld number with L/D ratios 0.5, 1.0 and1.5 respectively is shown in fig.15. It is observed that the whirl ratio remains constant at higher L/D ratios and decreasing exponentially with the increase in Sommerfeld number, which indicates better stability from the view point of whirl motion. It can be seen that the whirling frequency ratio equals to 0.5 at all aspect ratio. The similar trend in the value of whirl ratio parameter was reported in ref. [1]. Fig.16 shows variation of the stability threshold speed with respect to Sommerfeld number with L/D ratios 0.5, 1.0 and1.5 respectively. The value of stability threshold speed is increased with decrease in L/D ratio. This is due to the variation in the value of pressure gradients changes, and hence the value of bearing dynamic coefficient gets altered. Thus, the bearing stability threshold speed margin is expected to change. The similar trend in the value of threshold speed parameter was reported in ref. [7].

Fig.15. Whirl ratio versus Sommerfeld number

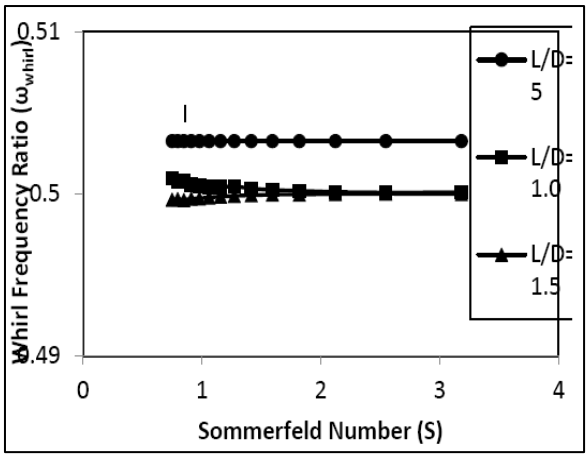

Fig.16. Threshold Speed Versus Sommerfeld Number

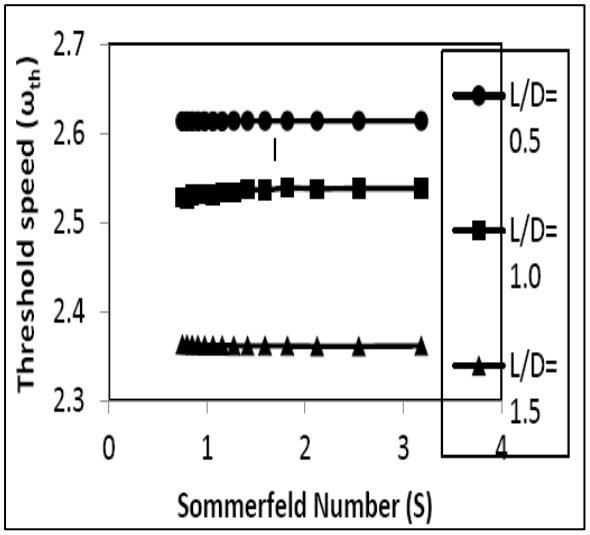

Fig.17 Critical Mass Parameter Versus Sommerfeld Number

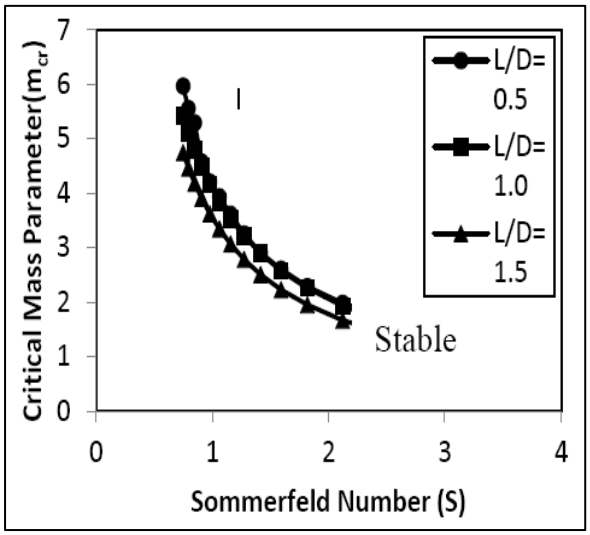

Fig.17 shows critical mass parameter, which is also an indicator of stability of hydrodynamic journal bearings. The lower and upper sides of each curve correspond to stable and unstable regions, respectively. It is observed that the stability of hydrodynamic journal bearings deteriorates with an increase in L/D ratio. The similar trend in the value of critical mass parameter was reported in in ref. [7, 8].

4.0 Conclusions

This study investigates the effect of aspect ratio on the performance of hydrodynamic bearings. Based on results, following conclusions can be drawn for a plane circular hydrodynamic bearing.

1) The minimum fluid- film thickness, attitude angle, coefficient of friction, Sxz, damping coefficient (Cxx, Czz and Cxz) increases with increase in L/D ratio.
2) The eccentricity ratio, maximum pressure, direct stiffness coefficient, Szx, Critical mass parameter decreases with increases in L/D ratio.
3) The value of threshold speed is increases with decrease in L/D ratio.
4) The whirling frequency ratio is independent of L/D ratio and always equals to or approximate to 0.5. The high-frequency whirling frequency ratio is decreasing exponentially with the increase in Sommerfeld number.
5) The stability of hydrodynamic journal bearings deteriorates with an increase in L/D ratio.

Nomenclature

Dimensional Parameters

c	: Radial clearance, mm
C_{ij}	: Fluid-film damping coefficients $(i,j = x,z)$, N.mm^{-2}
D	: Journal diameter, mm
e	: Journal eccentricity, mm
ε	: eccentricity ratio, e/c
F	: Fluid-film reaction ($\partial h/\partial t \neq 0$), N
F_x, F_z	: Fluid-film reaction components in X and Y direction ($\partial h/\partial t \neq 0$), N
h	: Nominal fluid-film thickness, mm
L	: Bearing length, mm
M_c, M_J	: Critical mass and Mass of journal, Kg
N	: Rotational speed, rpm
O_B	: Center of the bearing
O_j	: Center of the journal
p	: Pressure, N.mm^{-2}

p_s : Reference pressure, N.mm^{-2} ($\mu_r \omega_J R_J^{\ 2} / c^2$)

r : Radial coordinate

R, R_b : Radius of journal and bearing, mm

S : Sommerfeld Number

S_{ij} : Fluid-film stiffness coefficients ($i, j = x, z$), N.mm^{-1}

τ : Time, sec

W : load Capacity, N

W_o : External load, N

x : Circumferential coordinate

y : Axial coordinate

X_J, Z_J : Journal center coordinate

X, Y, Z : Cartesian coordinate system

z : Coordinate along film thickness

Greek Letters

μ : Lubricant viscosity, Pa. sec

ρ : Density, Kg.m^{-3}

α : Angular coordinate, rad

ϕ : Attitude angle, rad

ω_{th} : Threshold speed, rad.sec^{-1}

ω_{whirl} : Whirl frequency, rad-sec^{-1}

1.1. Non-Dimensional Parameters

$$\overline{C}_{ij} = C_{ij}\left(\frac{c^3}{\mu_r R_J^4}\right)$$

$$\overline{F}_x, \overline{F}_z = (F_x, F_z / p_s R_j^2)$$

$$\overline{h} = h/c$$

$$\overline{h}_{\min} = h_{\min}/c$$

$$\overline{p} = (p/p_s)$$

$$\overline{p}_L, \overline{p}_{\max} = (p_L, p_{\max})/p_s$$

$$\overline{S}_{ij} = S_{ij}\left(\frac{c}{p_s R_J^2}\right)$$

$$\overline{t} = t\left(c^2 p_s / \mu_r R_J^{\ 2}\right)$$

$$\overline{W}_o = \frac{W_o}{p_s R_J^2}$$

$$(\overline{X}_J, \overline{Z}_J) = (X_J, Z_J)/c$$

$$(\overline{X}, \overline{Z}) = (X, Z)/c$$

$$\alpha, \beta = (x, y)/R_J$$

$$\varepsilon = e/c$$

L/D = Aspect ratio

$\overline{\omega}_{th} = \omega_{th}/\omega_J$

$\overline{\omega}_{whirl} = \omega_{whirl}/\omega_J$

$\Omega = \omega_J\left(\mu_r R_J^2 / c^2 p_s\right)$, Speed parameter

Matrices

$[\overline{F}]$ = Assembled Fluidity Matrix,

$\{\overline{p}\}$ = Nodal pressure Vector,

$\{\overline{Q}\}$ = Nodal Flow Vector,

$\{\overline{R}_H\}$ = Column Vectors due to hydrodynamic terms,

$\{\overline{R}_{X_J}\}, \{\overline{R}_{Z_J}\}$ =Global right hand side vectors due to journal center linear velocities.

Subscripts and Superscript

b : Bearing

J : Journal

max : Maximum value

min : Minimum value

x,y,z : Components in X, Y and Z directions

. : First derivative w.r.t. time

References

[1] Zhang WM, BinZhou J and Meng J, Performance and stability analysis of gas-lubricated journal bearings in MEMS, Tribology International 2011;44:887-897.

[2] Das S, Guha SK and Chattopadhyay AK, Linear stability analysis of hydrodynamic journal bearings under micropolar lubrication, Tribology International 2005;38:500-507.

[3] Osman TA, Nada GS and Safar ZS, Static and dynamic characteristics of magnetized journal bearings lubricated with ferrofluid, Tribology International 2001;34:369-380.

[4] Zhang X, Yin Z, Gao G and ZhengLi, Determination of stiffness coefficients of hydrodynamic water-lubricated plain journal bearings, Tribology International 2015;85:37-47.

[5] Singhal S and Khonsari MM, A simplified Thermohydrodnamic Satbility Analysis of Journal Bearings Proc., IMechE 2005;219:225-234.

[6] Jang GH and Yoon JW, Stability analysis of a Hydrodynamic journal Bearing with Rotating Herringbone Grooves ASME Jr. of Tribology 2003;125:291-300.

[7] Sharma S and Krishna CM, Effect of L/D Ratio on the Performance of Two-Lobe Pressure Dam Bearing: Micropolar Lubricated, Advances in Tribology 2015; 1-7.

[8] Dwivedi VK, Chand S, and Pandey KN, Effect of different flow regime on the static and dynamic performance parameter of hydrodynamic bearing, Procedia Engineering 2013;51:520-528.

[9] Mehta NP, Rattan SS, and Bhushan G, Static and dynamic characteristics of four-lobe pressure-dam bearings, Tribology Letters 2003; 15:415.

[10] Smith DM, Journal Bearing in Turbo machinery, Chapman and Hall Ltd 1969.

[11] Balupari RS,Validation of Finite Element Program For Journal Bearings Static and Dynamic Properties-Thesis, University of Kentucky 2004.

[12] Sharma RS, Chand S and Jain SJ, Performance Characteristics of Externally Pressurized Orifice Compensated Flexible Journal Bearing, STLE Tribology Transaction 1991;34:465-471.

[13] Sharma SC, Kumar V, Jain SC, Sinhasan R and Subramanian M, A Study of Slot-Entry Hydrostatic/Hybrid Journal Bearing using the Finite Element Method, Tribology International 1999;32:185-196**.**

[14] Sharma SC, Jain SC and Reddy NMM, A study of Non-recessed Hybrid Flexible Journal Bearing with Different Restrictors, STLE Tribology Transaction 2001;44(2):310-317.

[15] Chandrawat HN and Sinhasan R, A Study of Steady State and Transient Performance Characteristics of Flexible Shell Journal Bearing, Tribology International 1988;21:137-148.

[16] Awasthi RK, The influence of wear and running-in on fluid-film journal bearing system -Thesis, Department of mechanical and industrial engineering ,Indian institute of technology roorkee, India 2006.